Supporting Information

Ag_2S Quantum Dot: A Bright and Biocompatible Fluorescent Nanoprobe in the Second Near-Infrared Window

Yan Zhang[1$], Guosong Hong[2$], Yejun Zhang[1$], Guangcun Chen[1], Feng Li[1], Hongjie Dai[2]*, and Qiangbin Wang[1]*

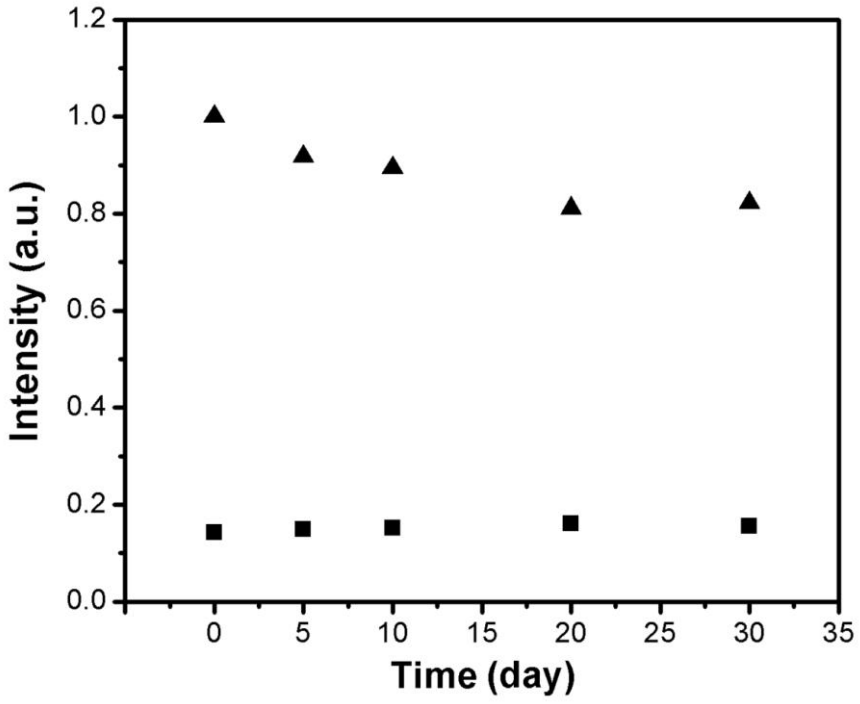

Figure S1. The photostability of the as-prepared original hydrophobic 5.4 nm Ag_2S QDs (▲) and the hydrophilic DHLA-Ag_2S QDs after ligand-exchange (■) in 30 days. It was observed that the PL intensity of the hydrophobic Ag_2S QDs was stabilized at 85 % of its original PL intensity in 30 days and the PL intensity of the hydrophilic Ag_2S QDs kept constant in 30 days. It was noticeable that the PL intensity of Ag_2S QDs decreased 7 times after the ligand-exchange process, which is similar to the behavior of CdSe QDs. This figure was plotted by normalizing the PL intensity of the hydrophilic DHLA-Ag_2S QDs (■) to the hydrophobic Ag_2S QDs (▲).

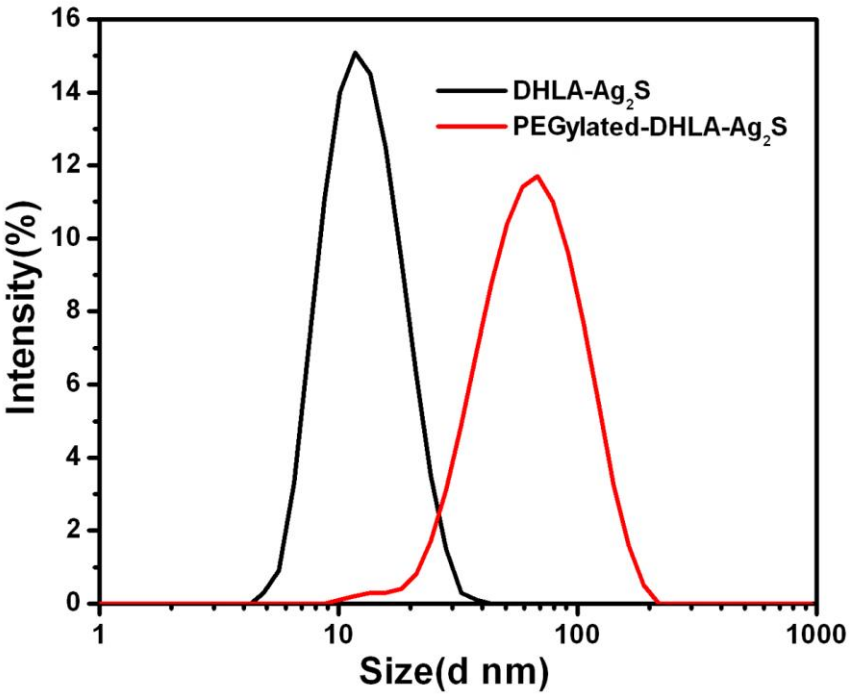

Figure S2. The hydrodynamic diameters of DHLA-Ag_2S QDs and PEGylated- DHLA-Ag_2S QDs. The average hydrodynamic diameter of DHLA-Ag_2S and PEGylated-DHLA-Ag_2S is 11.8 nm and 56.53 nm, respectively.

		Mean (mV)	Area (%)	Width (mV)
Zeta Potential (mV): -29.1	Peak 1:	-29.1	100.0	3.94
Zeta Deviation (mV): 3.94	Peak 2:	0.00	0.0	0.00
Conductivity (mS/cm): 2.49	Peak 3:	0.00	0.0	0.00

Result quality : Good

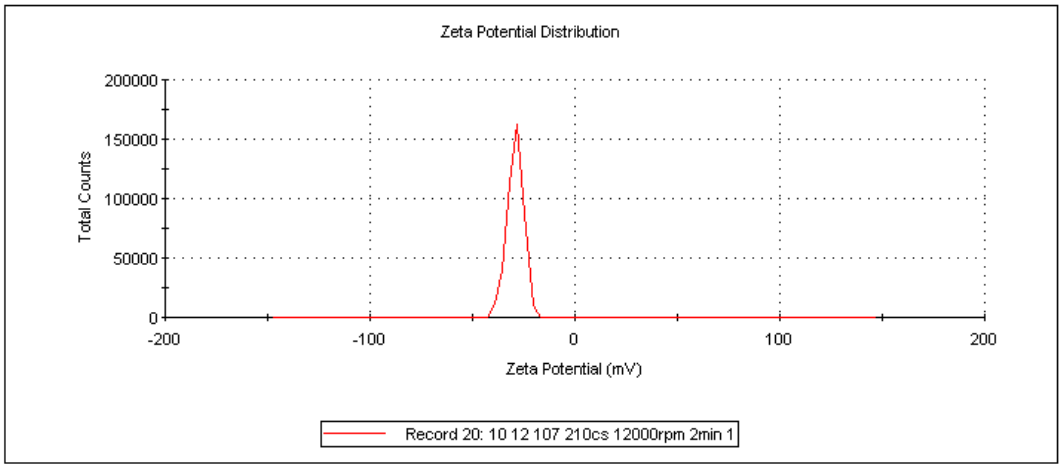

Figure S3. Zeta potential of DHLA-Ag_2S QDs (-29.1 mV).

		Mean (mV)	Area (%)	Width (mV)
Zeta Potential (mV): 3.93	Peak 1:	3.93	100.0	6.03
Zeta Deviation (mV): 6.03	Peak 2:	0.00	0.0	0.00
Conductivity (mS/cm): 0.0622	Peak 3:	0.00	0.0	0.00

Result quality : See result quality report

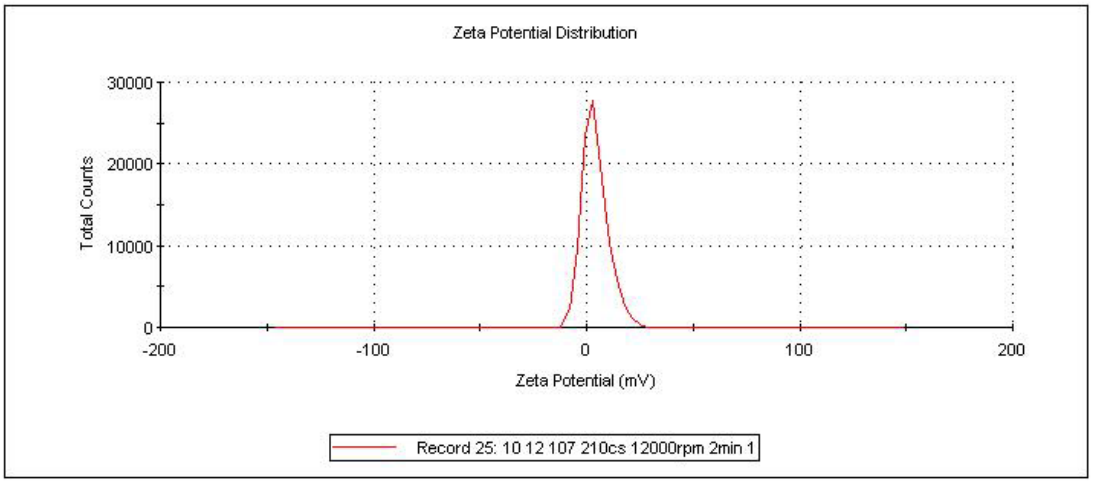

Figure S4. Zeta potential of PEGylated-DHLA-Ag_2S QDs (3.93 mV).

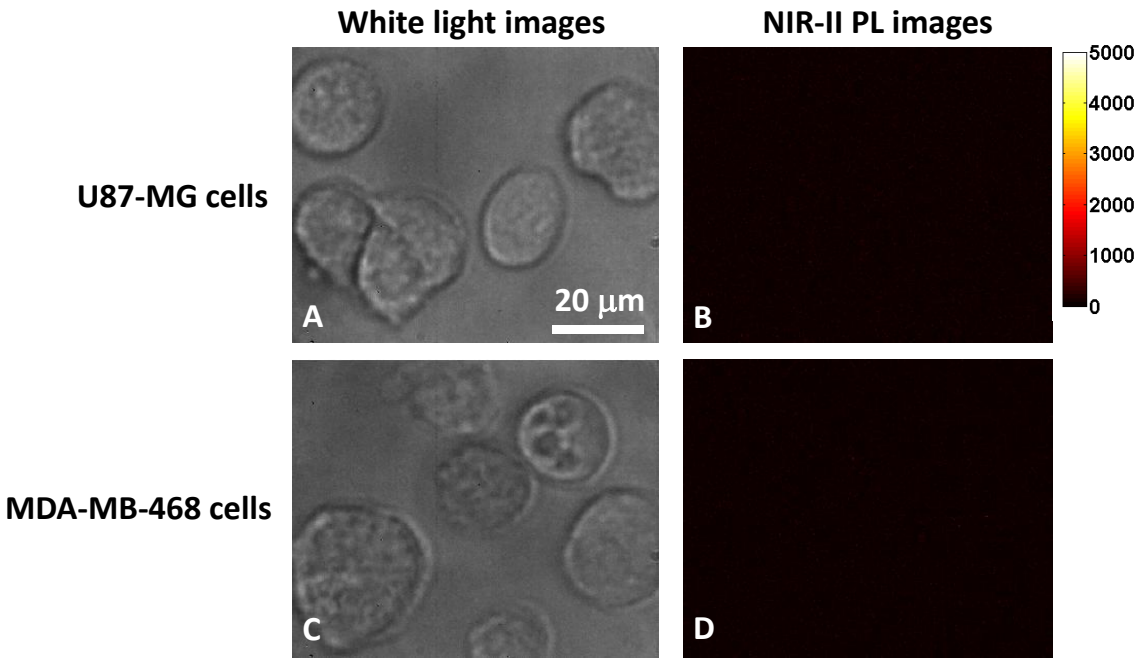

Figure S5. Negative control experiment of U87-MG and MDA-MB-468 cells stained with target-free, DHLA-Ag_2S QDs. White light optical image (A) and NIR-II PL image (B) of U87-MG cells incubated in the presence of DHLA-Ag_2S QDs. White light optical image (C) and NIR-II PL image (D) of MDA-MB-468 cells incubated in the presence of DHLA-Ag_2S QDs.

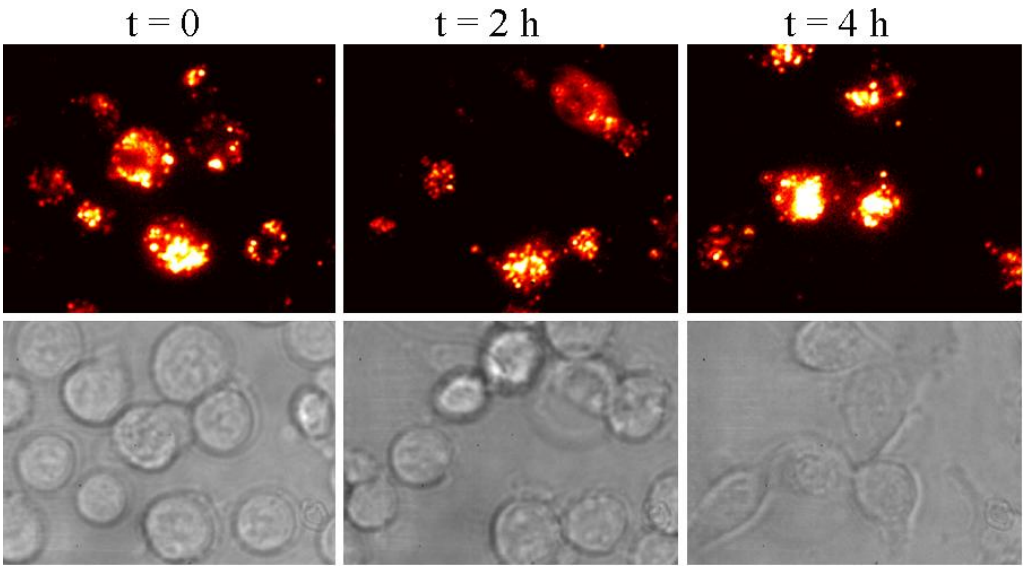

Figure S6. Long time *in situ* imaging of DHLA-Ag_2S QD/RGD stained U87 MG cells at 37 ℃ with CO_2 flow of 0.4 L/min in cell medium.

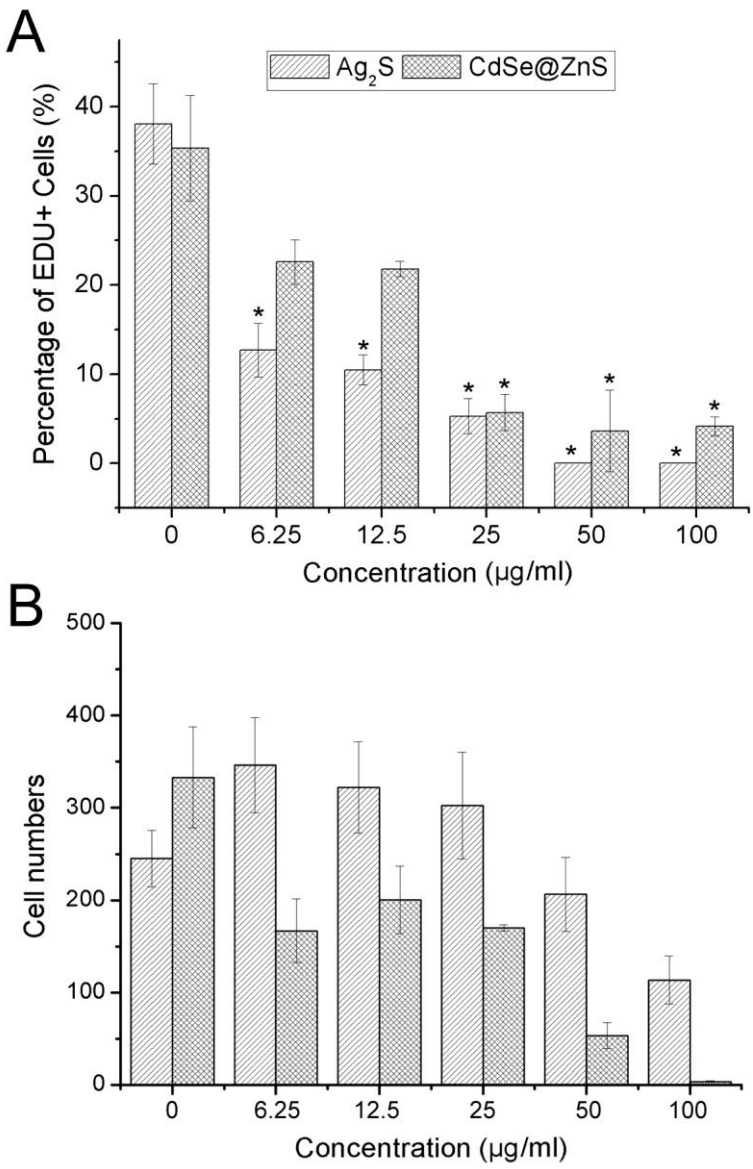

Figure S7. Effect of DHLA-Ag_2S and MPA-CdSe@ZnS QDs on the U87 MG cells proliferation (*: $P < 0.05$) (A) and the counted cells number (B) after 72 h treatment. From Figure S7A, it seemed that the DHLA-Ag_2S QDs possess higher cytotoxicity in comparison with MPA-CdSe@ZnS QDs. However, it was not the truth. When we counted the cells number after incubating the U87 MG cells with DHLA-Ag_2S and MPA-CdSe@ZnS QDs at different concentrations for 72 h, it was found that that most of the cells incubated with MPA-CdSe@ZnS QDs were killed at high concentrations such as 50 and 100 μg/mL. Instead, the live cells remained a much higher population in case of incubating with DHLA-Ag_2S under the same conditions.

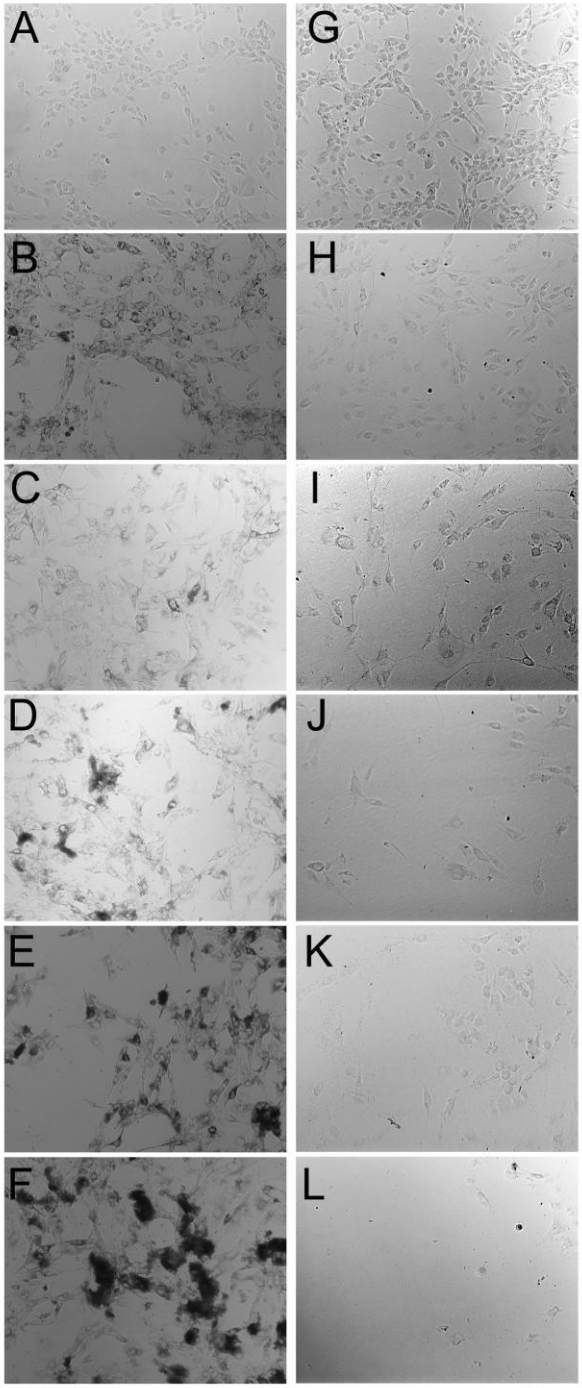

Figure S8. Optical images of U87 MG cells incubated with DHLA-Ag_2S (A-F: 0, 6.25, 12.5, 25, 50, and 100 μg/mL) and MPA-CdSe@ZnS QDs (G-L: 0, 6.25, 12.5, 25, 50, and 100 μg/mL) after 72 h treatment. The cell culture media of DMEM caused the severe precipitation of DHLA-Ag_2S surrounding the U87 MG cells, which resulted in that the U87 MG cells were treated at a much higher concentration of Ag_2S indeed. So, what the truth is that the proliferation data in Figure S7A were underrated.

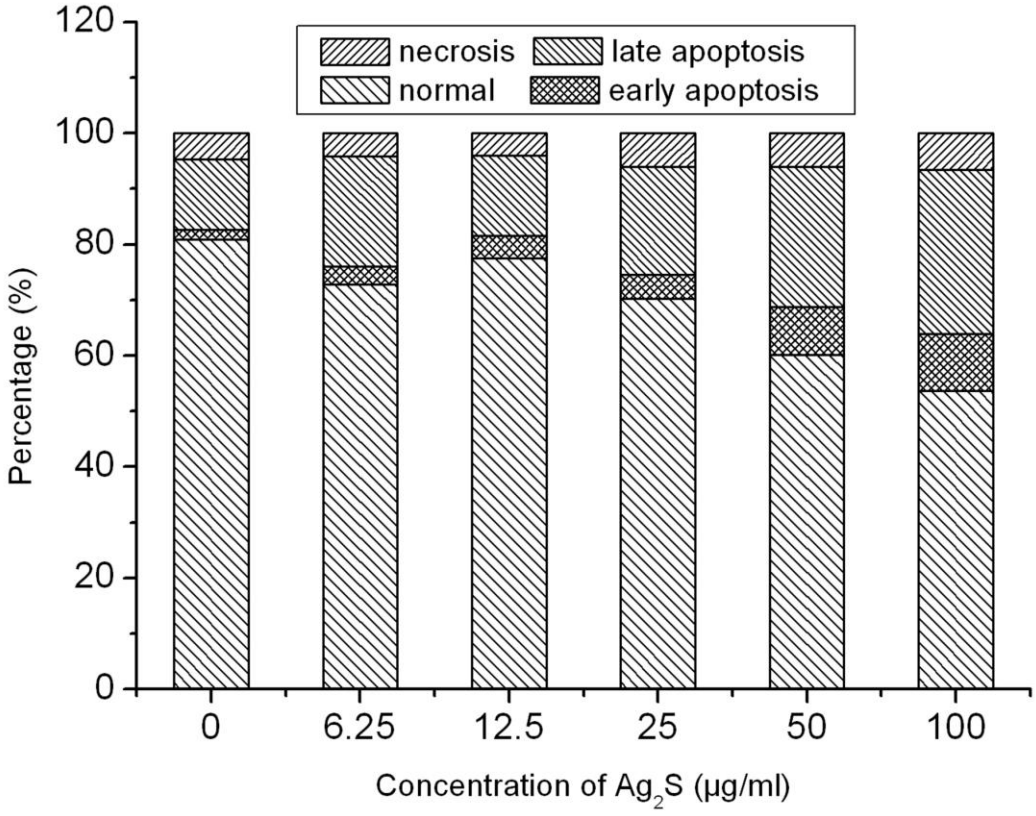

Figure S9. Effect of DHLA-Ag_2S on the apoptosis and necrosis of U87 MG cells after 72 h treatment.

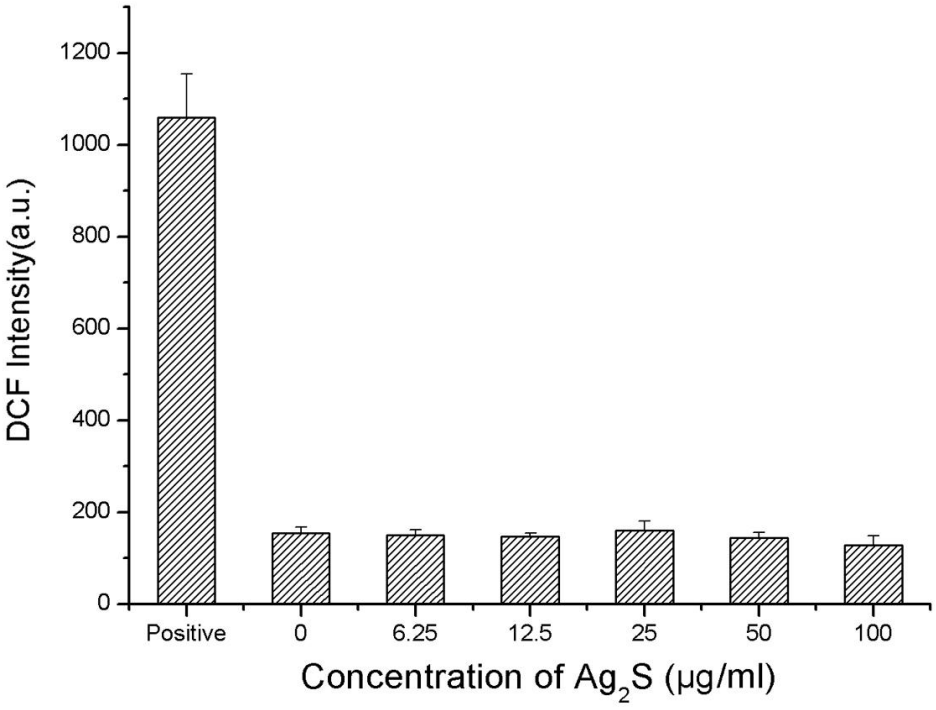

Figure S10. Effect of DHLA-Ag_2S on the ROS production of U87 MG cells after 72 h treatment.

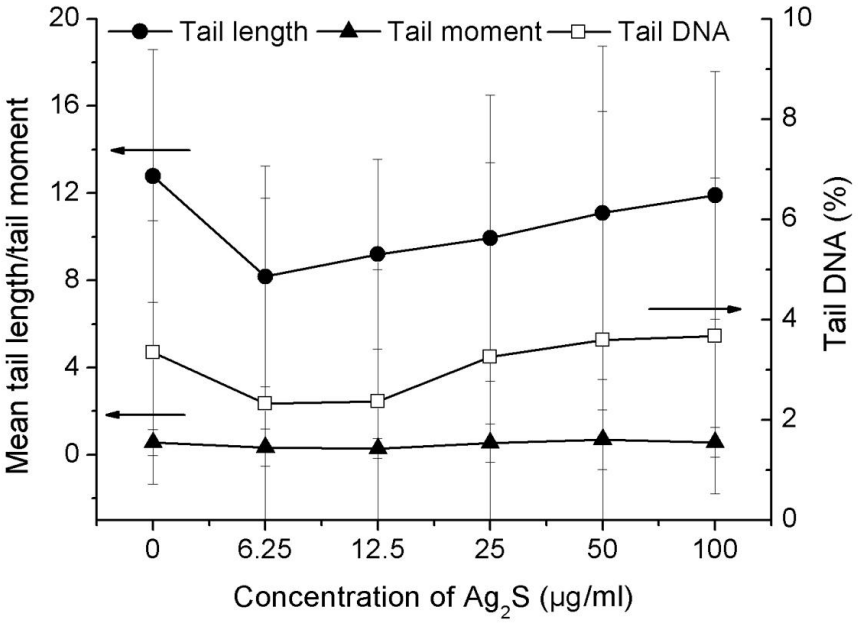

Figure S11. Comet assay of DHLA-Ag_2S on the U87 MG cells after 72 h treatment.

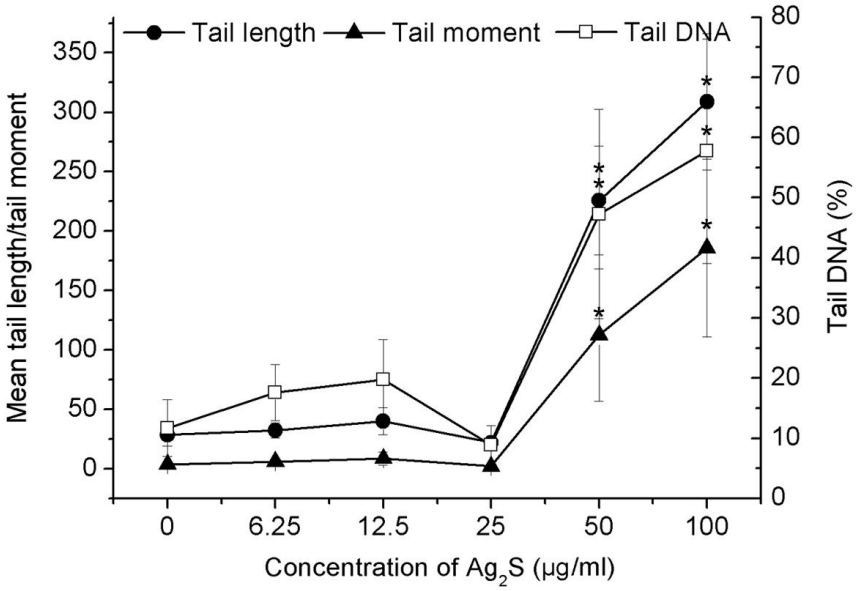

Figure S12. Comet assay of MPA-CdSe@ZnS QDs on the L929 cells after 72 h treatment (*: $P < 0.05$).

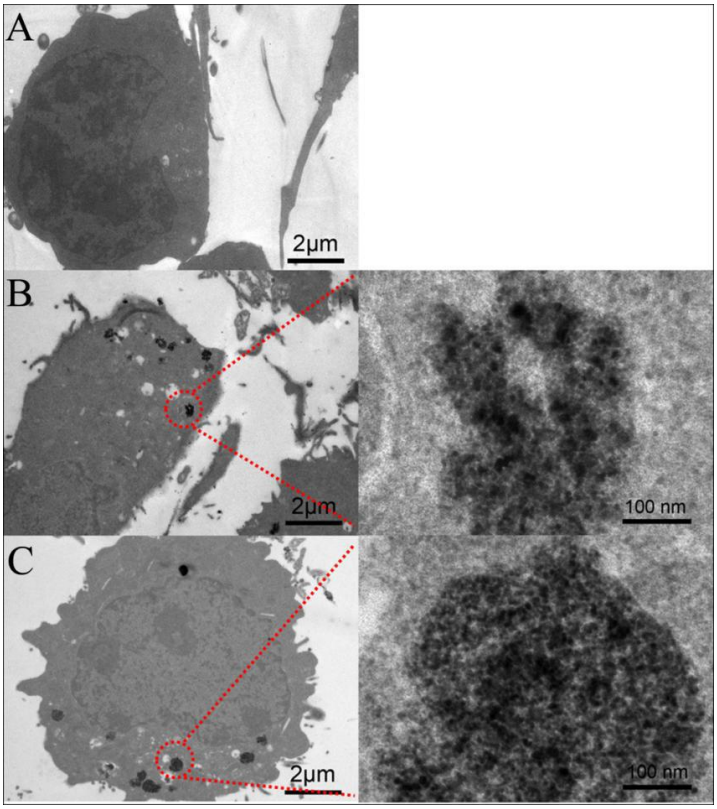

Figure S13. TEM images of the uptake of Ag_2S by L929 cell at different concentrations. A: 0 μg/mL; B: 12. 5 μg/mL; C: 100 μg/mL.